2014 IEEE International Conference on Fuzzy Systems (FUZZ-IEEE)
July 6-11, 2014, Beijing, China

# Quantum-Inspired Multidirectional Associative Memory for Human-Robot Interaction System

Naoki Masuyama and Chu Kiong Loo

***Abstract*— Quantum-Inspired Computational Intelligence based on quantum postulates is an emerging research area that exploit the parallelism of quantum mechanics. However, existing research efforts are limited to theoretical simulations and has not been implemented in robot application. With regards as Human-Robot Interaction, associative memory become essential for mutual communication. However, associative memory always suffers from limited memory capacity and high sensitivity to noise and the ability to recall from multi-modal sensory inputs. In this paper, we propose a Quantum-Inspired Multidirectional Associative Memory. This is the first attempt to overcome these two problems effectively with robot application.**

## I. Introduction

In the near future, some countries will be faced with aging society [1]. In this situation, one of the most critical problems is the elderly people who are living alone will be increased. Due to lack of communication, they would be increased the probability of the cognitive decline, risk of the dementia and so on. Several communication robots have been proposed to improve this situation [2]. These robots, however, have quite limited communication abilities that compare with human. On the other hand, the robot that has human-like body has been developed. It has the sufficient ability to perform active communication like human [3]. It can be approached the human-like communication.

The issue of social communication has been discussed in sociology, developmental psychology, relevance theory, and embodied cognitive science [4]. In the society of mind theory proposed by Minsky, intelligence is explained as a being combination of multiple simpler things. Each person has his/her own cognitive environment. One person can understand the meaning of an unknown word spoken by another because the person makes the symbol correspond to the percept. Such a shared cognitive environment is called a mutual cognitive environment [3]. Through the communication with human, the robot can understand personal preferences, interests and intentions. Conventionally, if the robot provides a topic, it is selected a suitable one based on past history of conversation with human, human behavior or general topics such as weather and news from the Internet. With regards as Human-Robot Interaction, associative memory become essential for mutual communication. If we apply multidirectional associative memory under shared cognitive environment, however, the robot can provide the more suitable topic of current content for conversation with human. As a result, communication with robot and human will be more mature.

Various types of associative memory have been proposed. In the early 1980's, Hopfield proposed an auto-associative memory model to store and recall information [5]. However, this model suffers from a lack of memory capacity and noise tolerance. In the late 1980's, Kosko extended the Hopfield model and introduced Bidirectional Associative Memory (BAM) [6]. However, the original Kosko BAM also suffers from low storage capacity and poor recall reliability. It has been shown that with $n$ neurons without noise, BAM's memory capacity does not exceed $0.15n$. Moreover, BAM is limited to"one to one" associations. To overcome this problem, Hagiwara proposed Multidirectional Associative Memory (MAM) in 1990 [7]. This model has multiple layers that are all connected. As a result of this layered architecture, MAM can handle "one to many" associations. The network structure of MAM is similar to BAM; thus, MAM also suffers from low memory capacity and poor noise tolerance. Conventionally, several methods have been proposed to improve the capacity of the associative memory model; for example, dummy neurons [8] and hidden layers [9] have been added, or each layer has been given a defined weight matrix [10]. Nevertheless, the memory capacity of these models remains limited. Hattori applied the Quick Learning algorithm to MAM [11]. This model improved both memory capacity and recall reliability. The recall process, however, takes much longer than the basic MAM. In early 2000's, Rigatos proposed the Quantum Mechanics Inspired Hopfield model [12]. This model demonstrats that quantum information processing in neural structures results in an exponential increase in storage capacity and can explain the extensive memorization and inferencing capabilities of humans. However, it is limited to auto-associative memory, and research efforts are limited to theoretical simulations and has not been implemented in robot application.

In this paper, we develop a theory for Quantum-Inspired Multidirectional Associative Memory (QMAM), and applying it to a interaction system with a robot. In section I I, first of all, we show the structure of QMAM. Next, we show similarity between Fuzzy inference and quantum mechanics in QMAM, and proof fuzzy inference satisfies two basic postulates of Quantum Mechanics. In section Ⅲ, we present simulation experiments about Memory Capacity and Noise Tolerance.In section Ⅳ, we explain computational intelligence for Robot Partner and the total architecture

Naoki Masuyama and Chu Kiong Loo are with Faculty of Computer Science and Information Technology, University of Malaya, 50603 Kuala Lumpur, Malaysia (email: naoki.masuyama17@siswa.um.edu.my, ckloo.um@um.edu.my).

The authors would like to acknowledge a scholarship provided by the University of Malaya (Fellowship Scheme). This research is supported by eScienceFund Project (01-01-03-SF0661) MOSTI, Malaysia.

of interaction system using QMAM. Section V presents the experimental results that communication between Robot Partner and human.

## II. Quantum Mechanics for Associative Memory

Superposition and unitarity are the key features of Quantum Mechanics. Superposition can be explained as "multiple states", which exist simultaneously in the Quantum System. The evolution of a closed Quantum System is described by a unitary transformation. If we apply fuzzy inference with same width triangular membership functions in weight matrix, it will be satisfied basic postulates of Quantum Mechanics as superposition and unitary operation. In QBAM, Unitarity is satisfied by rotations between spaces that are spanned by the eigenvectors of weight matrices. Rigatos showed avobe postulates with Hopfield model [12]. We extent it to multidirectional model. The mathematical proofs are presented from sessions $C$ to $F$.

### A. Fundamental Structure of Quantum Associative Memory

Here, we explain the structure of QMAM between $\alpha$-th layer and $\beta$-th layer. Equation structurs are following:

- $\alpha$-th layer to $\beta$-th layer

$$\begin{cases} X^{(k)}_{j(\alpha)} = \sum_{i=1}^{M} W^{(\alpha\beta)T}_{ij} x^{(k)}_{i(\alpha)} & \text{(1a)} \\ x^{(k)}_{j(\beta)} = \text{sgn}\left( \sum_{\substack{\alpha=1 \\ \alpha\neq\beta}}^{L} X^{(k)}_{j(\alpha)} \right) & \text{(1b)} \end{cases}$$

- $\beta$-th layer to $\alpha$-th layer

$$\begin{cases} X^{(k)}_{i(\beta)} = \sum_{j=1}^{N} W^{(\alpha\beta)}_{ij} x^{(k)}_{j(\beta)} & \text{(2a)} \\ x^{(k)}_{i(\alpha)} = \text{sgn}\left( \sum_{\substack{\beta=1 \\ \beta\neq\alpha}}^{L} X^{(k)}_{i(\beta)} \right) & \text{(2b)} \end{cases}$$

Let $\left\{ x^{(k)}_{(1)}, x^{(k)}_{(2)}, \ldots, x^{(k)}_{(L)} \right\}$, for $k = 1, 2, \ldots,$ be the bipolar pattern to be stored. $k$ denotes the number of pattern pairs, $L$ denotes the number of layers in QMAM, $M$ and $N$ denote the number of neurons in $\alpha$-th layer and $\beta$-th layer, respectively.

The waight matrix $W^{(\alpha\beta)T}$ and $W^{(\alpha\beta)}$ are as follows:

- $\alpha$-th layer to $\beta$-th layer

$$W^{(\alpha\beta)T} = \tfrac{1}{k} \sum_{g=1}^{k} x^{(g)T}_{(\beta)} x^{(g)}_{(\alpha)} \tag{3}$$

- $\beta$-th layer to $\alpha$-th layer

$$W^{(\alpha\beta)} = \tfrac{1}{k} \sum_{g=1}^{k} x^{(g)T}_{(\alpha)} x^{(g)}_{(\beta)} \tag{4}$$

where, $\alpha$ and $\beta$ denote the layer number, exponential $T$ denotes transpose. Here, $x$ is calculated by Gram-Schmidt orthogonalization that according to $\boldsymbol{a}_1 = \boldsymbol{A_1}/\|\boldsymbol{A_1}\|$ $(p = 1)$, $\boldsymbol{b}_p = \boldsymbol{A}_p - \sum_{i=p-1}^{k-1} (\boldsymbol{a}_i, \boldsymbol{A}_i)\, \boldsymbol{a}_i$ and $\boldsymbol{a}_p = \boldsymbol{b}_p/\|\boldsymbol{b}_p\|$ $(2 \leq p \leq k)$, where $\boldsymbol{A}$ denotes the vector of performing orthogonalization, $\boldsymbol{a}$ and $\boldsymbol{b}$ denote orthonormalized vector and orthogonalized vector as $x$, respectively. The each layer will be continued to cyclic update until it reaches the equilibrium state.

### B. Definision of Weight Matrix Update

Equations (5) and (6) show the update rules of weight matrix. Here, $t$ denotes time steps, exponential $T$ denotes transpose. $x^{(k)}_{(\alpha\text{-stored})}$ and $x^{(k)}_{(\beta\text{-stored})}$ denote $k$th stored pattern, and $x^{(k)}_{(\alpha)}$ and $x^{(k)}_{(\beta)}$ denote inner state of $\alpha$-th layer and $\beta$-th layer, respetively. $M$ and $N$ denote the number of neurons in $\alpha$-th layer and $\beta$-th layer, respectively. $F$ $(0 < F \leq 1)$ denotes variation amount in position for the center of Fuzzy triangular. The learning algorithm is refered from a general model for BAM (GBAM) [10]. This model tried to find a asymptotic stability condition of learning algorithm for improve its abilities. The fundamental update algorithm is based on Hebbian learning. Thus, we considered that it can be applied to proposed model.

### C. Similarity of Quantum Mechanics and Fuzzy Inference

In quantum mechanics, the state of an isolated quantum syste $Q$ is represented by a vector $|\psi_{(t)}\rangle$ in a Hilbert space. This vector satisfies Schrödinger's diffusion equation [13].

$$i\hbar \frac{d}{dt} |\psi_{(t)}\rangle = H\psi_{(t)} \tag{7}$$

where $H$ denotes Hamiltonian operator that gives the total energy $H = \left(p^2/2m\right) + V_{(x)}$. The probability to find the particle between $x$ and $x + dx$ at the time instant $t$,the wave function $\psi_{(x,t)}$ can be analyzed as follows in a set of orthonormal eigenfunctions in a Hilbert space: $\psi_{(x,t)} = \sum_{m=1}^{\infty} c_m \psi_m$. Here, the coefficients $c_m$ is an indication of the probability to describe the particle's position $x$ at time $t$ by the eigenfunction $\psi_m$. From Eq. (7), the average position of the particle is found to be

$$\langle x \rangle = \sum_{m=1}^{\infty} \|c_m\|^2 a_m \tag{8}$$

with $\|c_m\|^2$ denotes the probability that the particle's position be described by the eigenfunction $\psi_m$. When the position $x$ that can be taken is the associated eigenvalue $a_m$. The eigenvalue $a_m$ is chosen with probability $P \propto \|c_m\|^2$.

In the same way, the probability to find the particle between $y$ and $y + dy$ at the time instant $t$ is given by $P_{(y)}dy = \left|\psi_{(y,t)}\right|^2$, then derived the following:

$$\langle y \rangle = \sum_{n=1}^{\infty} \|c_n\|^2 b_n \tag{9}$$

with $\|c_n\|^2$ denotes the probability that the particle's position be described by the eigenfunction $\psi_n$.

It is assumed that the Fuzzy variable $x$ and $y$ belong to a universe of discourse, that is quantized to an infinite number of Fuzzy sets $A_i, A_{-i}$ $(i = 1, 2, \ldots, \infty)$ and $B_j, B_{-j}$ $(j = 1, 2, \ldots, \infty)$, e.g. the axis of real number $R$ is partitioned to an infinite number of Fuzzy sets with the same space and width. The Fuzzy sets have the following properties:

(a) They satisfy

• $\alpha$-th layer to $\beta$-th layer

$$W_{ij}^{(\alpha\beta)T(t+1)} = \begin{cases} W_{ij}^{(\alpha\beta)T(t)} + \begin{cases} -F, & \text{If } x_{(\beta\text{-stored})}^{(k)} \sum_{i=1}^{M} W_{ij}^{(\alpha\beta)T(t)} x_{(\alpha)}^{(k)} \leq 0 \text{ and } W_{ij}^{(\alpha\beta)T(t)} \geq 0 \\ F, & \text{If } x_{(\beta\text{-stored})}^{(k)} \sum_{i=1}^{M} W_{ij}^{(\alpha\beta)T(t)} x_{(\alpha)}^{(k)} \leq 0 \text{ and } W_{ij}^{(\alpha\beta)T(t)} < 0 \end{cases} \\ W_{ij}^{(\alpha\beta)T(t)}, \quad \text{Otherwise} \end{cases} \tag{5}$$

• $\beta$-th layer to $\alpha$-th layer

$$W_{ij}^{(\alpha\beta)(t+1)} = \begin{cases} W_{ij}^{(\alpha\beta)(t)} + \begin{cases} -F, & \text{If } x_{(\alpha\text{-stored})}^{(k)} \sum_{j=1}^{N} W_{ij}^{(\alpha\beta)(t)} x_{(\beta)}^{(k)} \leq 0 \text{ and } W_{ij}^{(\alpha\beta)(t)} \geq 0 \\ F, & \text{If } x_{(\alpha\text{-stored})}^{(k)} \sum_{j=1}^{N} W_{ij}^{(\alpha\beta)(t)} x_{(\beta)}^{(k)} \leq 0 \text{ and } W_{ij}^{(\alpha\beta)(t)} < 0 \end{cases} \\ W_{ij}^{(\alpha\beta)(t)}, \quad \text{Otherwise} \end{cases} \tag{6}$$

---

• $\alpha$-th layer to $\beta$-th layer

$$\sum_{m=1}^{\infty} \mu_{A_m(x)} = 1 \quad \left(W_{ij}^T \geq 0\right) \tag{10a}$$

$$\sum_{m=1}^{\infty} \mu_{A_{-m}(x)} = 1 \quad \left(W_{ij}^T < 0\right) \tag{10b}$$

• $\beta$-th layer to $\alpha$-th layer

$$\sum_{n=1}^{\infty} \nu_{B_n(y)} = 1 \quad (W_{ij} \geq 0) \tag{11a}$$

$$\sum_{n=1}^{\infty} \nu_{B_{-n}(y)} = 1 \quad (W_{ij} < 0) \tag{11b}$$

(b) Each Fuzzy set $A_m$ and $B_n$ are described by its center $a_m$, $b_n$ and its width $F$.
(c) The average value of variable $x$ and $y$ will be given by:
• $\alpha$-th layer to $\beta$-th layer

$$\langle x \rangle = \sum_{m=1}^{\infty} \mu_{A_m(x)} a_m \quad \left(W_{ij}^T \geq 0\right) \tag{12a}$$

$$\langle x \rangle = \sum_{m=1}^{\infty} \mu_{A_{-m}(x)} a_{-m} \quad \left(W_{ij}^T < 0\right) \tag{12b}$$

• $\beta$-th layer to $\alpha$-th layer

$$\langle y \rangle = \sum_{n=1}^{\infty} \nu_{B_n(y)} b_n \quad (W_{ij} \geq 0) \tag{13a}$$

$$\langle y \rangle = \sum_{n=1}^{\infty} \nu_{B_{-n}(y)} b_n \quad (W_{ij} < 0) \tag{13b}$$

*D. Hebbian Learning Inspired Fuzzy Inference*

• $\alpha$-th layer to $\beta$-th layer

In Fig. 1(a), $A_1$, $A_2$, …, $A_{m-1}, A_m$ and $A_{-1}$, $A_{-2}$, …, $A_{-m+1}$, $A_{-m}$ are the Fuzzy subsets in which the universe of discourse of the variable $w_{ij}^T$. The sets $A_i$ and $A_{-i}$ are selected to have the same spread and to satisfy the strong Fuzzy partition equality $\sum_{i=1}^{m} \mu_{A_m(x)} = 1$ and $\sum_{i=1}^{m} \mu_{A_{-m}(x)} = 1$, respectively.

• $\beta$-th layer to $\alpha$-th layer

In Fig. 1(b), $B_1$, $B_2$, … , $B_{n-1}$, $B_n$ and $B_{-1}$, $B_{-2}$, … , $B_{-n+1}$, $B_{-n}$ are the Fuzzy subsets in which the universe of discourse of the variable $w_{ij}$. The sets $B_j$ and $B_{-j}$ are selected to have the same spread and to satisfy the strong Fuzzy partition equality $\sum_{j=1}^{n} \nu_{B_n(y)} = 1$ and $\sum_{j=1}^{n} \nu_{B_{-n}(y)} = 1$, respectively.

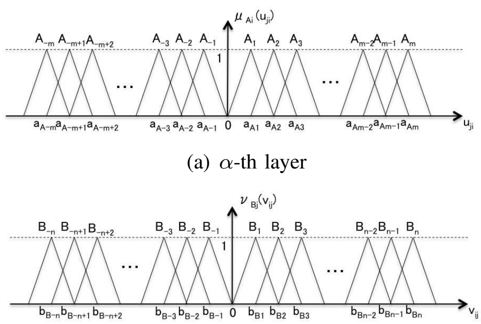

(a) $\alpha$-th layer

(b) $\beta$-th layer

Fig. 1: The Fuzzy set in $\alpha$-th layer and $\beta$-th layer.

The fuzzifier is selected to be a triangular one. The main t-norm is used for derivation of the Fuzzy relational matrices $R_m^i$ and $R_m^d$ ($\alpha$-th layer), $R_n^i$ and $R_n^d$ ($\beta$-th layer), where exponential "$i$" and "$d$" denotes "*increase*" and "*decrease*", respectively. These matrices have the following properties: In $\alpha$-th layer to $\beta$-th layer, $A_m = R_m^i \circ A_{m-1}$,$A_{m-1} = R_m^d \circ A_m$ ($W_{ij}^T \geq 0$), and $A_{-m} = R_{-m}^i \circ A_{-m+1}$, $A_{-m+1} = R_{-m}^d \circ A_{-m}$ ($W_{ij}^T < 0$). In $\beta$-th layer to $\alpha$-th layer, $B_n = R_n^i \circ B_{n-1}$, $B_{n-1} = R_n^d \circ B_n$ ($W_{ij} \geq 0$), and $B_{-n} = R_{-n}^i \circ B_{-n+1}$, $B_{-n+1} = R_{-n}^d \circ B_{-n}$ ($W_{ij} < 0$).

The max-min inference is used, while the defuzzifier is a center of average one. The learning algorithm is inspired from Hebbian learning and in the case of binary memory vectors $x_k$ and $y_k$ can be stated as follows:

• $\alpha$-th layer to $\beta$-th layer

$$\text{IF } x_k \sum_{i=1}^{m} W_{ij}^T x_i^k \leq 0 \text{ and } W_{ij}^T < 0, \text{ THEN increase } W_{ij}^T \tag{14a}$$

$$\text{IF } x_k \sum_{i=1}^{m} W_{ij}^T x_i^k \leq 0 \text{ and } W_{ij}^T \geq 0, \text{ THEN decrease } W_{ij}^T \tag{14b}$$

• $\beta$-th layer to $\alpha$-th layer

$$\text{IF } y_k \sum_{j=1}^{n} W_{ij} y_j^k \leq 0 \text{ and } W_{ij} < 0, \text{ THEN increase } W_{ij} \tag{15a}$$

$$\text{IF } y_k \sum_{j=1}^{n} W_{ij} y_j^k \leq 0 \text{ and } W_{ij} \geq 0, \text{ THEN decrease } W_{ij} \tag{15b}$$

The weight matrix update with above Fuzzy learning algorithm results by Fuzzy weight matrices. The latter can be decomposed into a superposition of associative memories. The whole associative memories $W^T$ and $W$ equals a weighted averaging of the individual weight matrices $\bar{W}^T$ and $\bar{W}$, i.e.

• $\alpha$-th layer to $\beta$-th layer

$$W^T = \sum_{i=1}^{2^M} \mu_i \bar{W}_i^T \tag{16}$$

• $\beta$-th layer to $\alpha$-th layer

$$W = \sum_{j=1}^{2^N} \nu_j \bar{W}_j \tag{17}$$

where, the non-negative weights $\mu_i$ and $\nu_j$ indicate the contribution of each local associative memory$\bar{W}_i^T$ and $\bar{W}_j$. $M$ and $N$ denote the number of neurons in $\alpha$-th layer to $\beta$-th layer, respectively.

### E. Fuzzy Inference is Performed through Unitary Operators

It will be shown that the increase and decrease Fuzzy operators that were described in the rule-base are unitary.

• $\alpha$-th layer to $\beta$-th layer

The Fuzzy relational matrices $R_i$ ($W_{ij}^T \geq 0$), $R_{-i}$ ($W_{ij}^T < 0$) used by increase and decrease Fuzzy operators satisfy the following Fuzzy relational equations, respectively:

(1) Increase mode:

(a) $W_{ij}^T \geq 0$ :

$$A_2 = R_1^i \circ A_1, A_3 = R_2^i \circ A_2, \ldots, A_m = R_{m-1}^i \circ A_{m-1} \tag{18a}$$

(b) $W_{ij}^T < 0$ :

$$A_{-2} = R_{-1}^i \circ A_{-1}, A_{-3} = R_{-2}^i \circ A_{-2}, \ldots, A_{-m} = R_{-m+1}^i \circ A_{-m+1} \tag{18b}$$

(2) Decrease mode:

(a) $W_{ij}^T \geq 0$ :

$$A_1 = R_1^d \circ A_2, A_2 = R_2^d \circ A_3, \ldots, A_{m-1} = R_{m-1}^d \circ A_m \tag{19a}$$

(b) $W_{ij}^T < 0$ :

$$A_{-1} = R_{-1}^d \circ A_{-2}, A_{-2} = R_{-2}^d \circ A_{-3}, \ldots, A_{-m+1} = R_{-m+1}^d \circ A_{-m} \tag{19b}$$

In both cases, "$\circ$" denotes the max-min operation. Substituting $A_{m-1} = R_{m-1}^d \circ A_m$ in $A_m = R_{m-1}^i \circ A_{m-1}$ one gets $A_m = R_{m-1}^i \circ \left(R_{m-1}^d \circ A_m\right)$, in the same way, $A_{-m} = R_{-m+1}^i \circ \left(R_{-m+1}^d \circ A_{-m}\right)$, and using the associativity of the max-min operator yields $A_m = \left(R_{m-1}^i \circ R_{m-1}^d\right) \circ A_m$, $A_{-m} = \left(R_{-m+1}^i \circ R_{-m+1}^d\right) \circ A_{-m}$, respectively, i.e.

$$\begin{cases} \left(R_{m-1}^i \circ R_{m-1}^d\right) = I & (20a) \\ \left(R_{-m+1}^i \circ R_{-m+1}^d\right) = I & (20b) \end{cases}$$

Setting $A_m = R_{m-1}^i \circ A_{m-1}$ in $A_{m-1} = R_{m-1}^d \circ A_m$, $A_{-m} = R_{-m+1}^i \circ A_{-m+1}$ in $A_{-m+1} = R_{-m+1}^d \circ A_{-m}$, and using the associativity of the max-min operation yields $A_{m-1} = \left(R_{m-1}^d \circ R_{m-1}^i\right) \circ A_{m-1}$, $A_{-m+1} = \left(R_{-m+1}^d \circ R_{-m+1}^i\right) \circ A_{-m+1}$, i.e.

$$\begin{cases} \left(R_{m-1}^d \circ R_{m-1}^i\right) = I & (21a) \\ \left(R_{-m+1}^d \circ R_{-m+1}^i\right) = I & (21b) \end{cases}$$

Furthermore, due to the generation of the matrices $R_{m-1}^i$ and $R_{m-1}^d$, $R_{-m+1}^i$ and $R_{-m+1}^d$ using Mandanis inference system, it holds the following relation:

$$\begin{cases} R_{m-1}^d = \left(R_{m-1}^i\right)^T & (22a) \\ R_{-m+1}^d = \left(R_{-m+1}^i\right)^T & (22b) \end{cases}$$

From (21a) and (22a), (21b) and (22b) are deduced following:

$$\begin{cases} \left(R_{m-1}^d\right)^{-1} = \left(R_{m-1}^i\right)^T & (23a) \\ \left(R_{-m+1}^d\right)^{-1} = \left(R_{-m+1}^i\right)^T & (23b) \end{cases}$$

Therefore, the increase and decrease operators are unitary.

• $\beta$-th layer to $\alpha$-th layer

In the same way as $\alpha$-th layer to $\beta$-th layer, the Fuzzy relational matrices $R_j$ $(W_{ij} \geq 0)$, $R_{-j}$ $(W_{ij} < 0)$ used by the increase and decrease Fuzzy operators satisfy Fuzzy relational equations. Therefore, same as $\alpha$-th layer to $\beta$-th layer, it will be derived following relationships:

$$\begin{cases} \left(R_{n-1}^d\right)^{-1} = \left(R_{n-1}^i\right)^T & (24a) \\ \left(R_{-n+1}^d\right)^{-1} = \left(R_{-n+1}^i\right)^T & (24b) \end{cases}$$

Therefore, the increase and decrease operators are unitary.

### F. Existence of Superposition in the Weight Matrix

• $\alpha$-th layer to $\beta$-th layer

Assume that weight element $w_{km}$ of matrix $W^T$, i.e. the element of the $k$th row and the $m$th column of $W^T$. Due to strong fuzzy partition, this weight belongs to two adjacent fuzzy sets $A_i$ and $A_{i+1}$. The corresponding centers of the fuzzy sets are $a_{km}^i$ and $a_{km}^{i+1}$, and because of the strong fuzzy partition, the associated memberships will be $\mu_{km} = \mu_{A_i}$ and $1 - \mu_{km} = \mu_{A_{i+1}}$. Therefore $w_{km}$ is described by the sets $\left\{\mu_{km}, a_{km}^{A_i}\right\}$ and $\left\{1 - \mu_{km}, a_{km}^{A_{i+1}}\right\}$. Taking the possible combinations of the memberships for each weight, the matrices that have as elements the memberships $\mu_{km}$, $1 - \mu_{km}$are generated. Taking the possible combinations of the projections of each weight to the centers of the adjacent fuzzy sets, the matrices that have as elements, the centers $a_{km}^{A_i}$ and $a_{km}^{A_{i+1}}$ are generated. Using the above, the decomposition of the weight matrix $W^T$ into the set of superimposing matrices $\bar{W}_i^T$ $\left(i = 1, 2, \ldots, 2^M\right)$.

TABLE I: Conditions for the Simulation of Memory Capacity.

| | | |
|---|---|---|
| Number of Pairs $k$ | : | 300 Pairs (Non Duplicates) |
| Neuron Representation | : | Bipolar |
| Data Set Configuration | : | Random Pattern |
| Variation $F$ | : | 0.005 |

| | No. of Layers | : | [1] | [2] | [3] | [4] | [5] |
|---|---|---|---|---|---|---|---|
| Number of Neurons | 5-Layers | condition (I-a) | 15 | 15 | 15 | 15 | 15 |
| | | condition (I-b) | 50 | 50 | 50 | 50 | 50 |
| | | condition (II-a) | 50 | 40 | 30 | 20 | 10 |
| | | condition (II-b) | 10 | 20 | 30 | 40 | 50 |

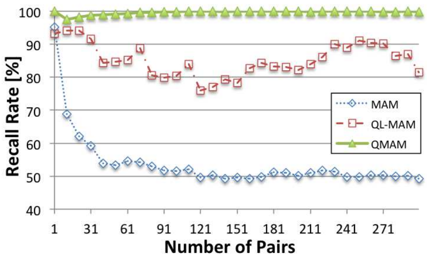


(a) condition (I-a)

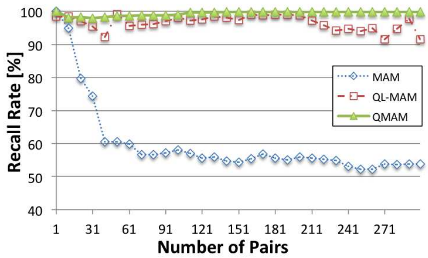


(b) condition (I-b)

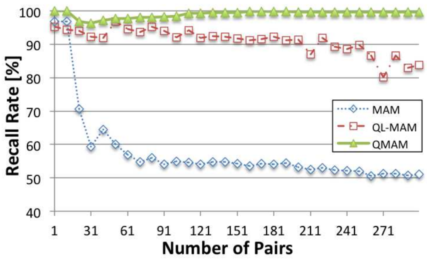


(c) condition (II-a)

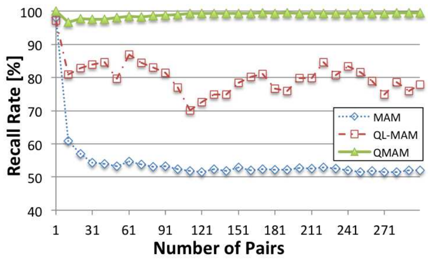


(d) condition (II-b)

Fig. 2: Results of Memory Capacity in 5-Layers with Constant Number of Neurons.

- $\beta$-th layer to $\alpha$-th layer

Assume that weight element $w_{kn}$ of matrix $W$, i.e. the element of the $k$th row and the $n$th column of $W$. Due to strong fuzzy partition, this weight belongs to two adjacent fuzzy sets $B_j$ and $B_{j+1}$. The corresponding centers of the fuzzy sets are $b_{kn}^{j}$ and $b_{kn}^{j+1}$, and because of the strong fuzzy partition, the associated memberships will be $\nu_{kn} = \nu_{B_j}$ and $1-\nu_{kn} = \nu_{B_{j+1}}$. Therefore $w_{kn}$ is described by the sets $\left\{\nu_{kn}, b_{kn}^{B_j}\right\}$ and $\left\{1-\nu_{kn}, \nu_{kn}^{B_{j+1}}\right\}$. Here, same as X-layer to Y-layer, the decomposition of the weight matrix $W$ into the set of superimposing matrices $\bar{W}_j \ \left(j = 1, 2, \ldots, 2^N\right)$.

## III. Simulation Experiment

In this section, we compare QMAM, MAM [7] and QL-MAM [11]. MAM is the fundamental model of multi-layer associative memory. QL-MAM is Quick Learning applied to MAM. This learning algorithm has improved weight matrices, Memory Capacity and Noise Tolerance. We conducted simulation experiments for (A) Memory Capacity, (B) Noise Tolerance and (C) Processing Time. In (A) and (B), we considered that if the correct recall rate for $k$ pattern pairs was over 90%, $k$ pattern pairs could be stored in memory.

### A. *Memory Capacity*

Memory Capacity is an important element of associative memory performance. This ability is affected by the number of neurons in each layer. In this section, we conducted experiments under two conditions. The first used the same number of neurons in each layer, the other used a different number of neurons in each layer.

Table I shows the experimental conditions. Here, "No. of Layers" means not only how many layers there were, but also represents recall order. These conditions demonstrate the effect of the number of neurons on Memory Capacity. A comparison of Figs. 2(a) and 2(b) shows that although the number of neurons is high, Fig. 2(b) shows a better recall rate than Fig. 2(a). In every condition QMAM has the highest recall rate and MAM the lowest. Moreover, a comparison of conditions (I) and (II) shows that for each condition, even when the number of neurons is small, QMAM has a higher recall rate than others. This result demonstrates that the Memory Capacity of QMAM is more robust than QL-MAM and MAM from the point of view of the number of neurons. In other words, QMAM has a relatively large Memory Capacity compared to QL-MAM and MAM, despite

TABLE II: SimulationConditions for Noise Tolerance.

| | | | | | | | |
|---|---|---|---|---|---|---|---|
| Neuron Representation | | : | Bipolar | | | | |
| Data Set Configuration | | : | Random Pattern | | | | |
| Noise Generation Method | | : | Random Generate | | | | |
| Variation Amount $F$ | | : | 0.005 | | | | |
| Number of Pairs $k$ | 5-Layers | condition (Ⅲ) | 20 | | | | |
| | | condition (Ⅳ) | 50 | | | | |
| | | condition (Ⅴ) | 150 | | | | |
| | No. of Layers | [1] | [2] | [3] | [4] | [5] | |
| Number of Neurons | 5-Layers | 50 | 45 | 40 | 35 | 30 | |

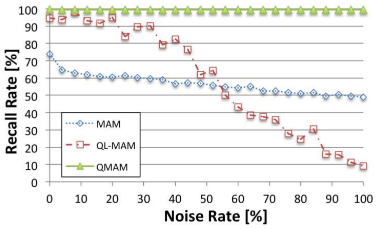


(a) condition (Ⅲ)

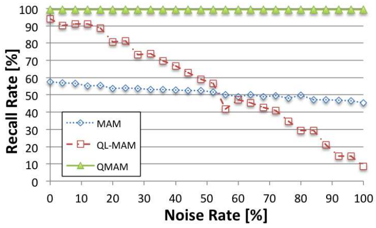


(b) condition (Ⅳ)

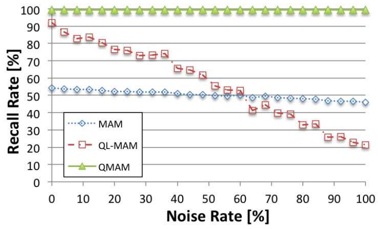


(c) condition (Ⅴ)

Fig. 3: Results of Noise Tolerance in 5-Layers with 3 conditions.

the lower number of neurons.

In addition, we conducted an experiment to demonstrate the effect on Memory Capacity of having different numbers of neurons in each layer. We anticipated that the magnitude of the difference in the number of neurons in each layer would have an effect on Memory Capacity. There is an interesting comparison with QL-MAM and MAM in Figs. 2(c) and 2(d); the recall rate is different, although the average number of neurons is the same. The cause of this effect seems to be the magnitude of the difference in the number of neurons in each layer. In both methods, the layer that has larger number of neurons is able to recall the layer that has the smaller number of neurons. On the other hand, the layer that has the smaller number of neurons cannot store the information contained in the layer that has the larger number of neurons. Although the same conditions with QMAM, it shows almost the same results between condition (Ⅱ-a) and (Ⅱ-b).

In summary, QMAM has a large Memory Capacity compared to conventional methods, and it remains robust in conditions where there are differences in the number of neurons in each layer.

### B. Noise Tolerance

Noise Tolerance is another significant function in associative memory. We measured Noise Tolerance by randomly adding noise to Layer No. [1]. We conducted experiments with different number of neurons in each layer of 3-Layers and 5-Layers simulations.

Table II shows the experimental conditions for Noise Tolerance. These conditions made it possible to measure differences in Noise Tolerance, depending on the number of stored patterns and layers. Fig. 2 shows that MAM cannot store any pattern pairs with $k = 20$ in 5-Layers. Thus, the MAM results shown in Fig. 3 has already converged to local minima. Fig. 3(a) shows that with a low noise rate the recall rate of QL-MAM is over 90%. However, as the noise rate increases, the correct recall rate decreases. On the other hand, QMAM has an almost 100% recall rate even when the noise rate is high.

### C. Processing Time

Processing Time is one of the critical problems for real-time application processing. Table III shows the Processing Time experimental conditions. QL-MAM and QMAM implement the learning algorithm for weight matrices. Thus, there are more recall process procedures for QMAM and QL-MAM than MAM.

Fig. 4 shows that QL-MAM processing time is greater than MAM. In contrast, QMAM Processing Time is only about 20% of MAM and 25% of QL-MAM. We argue that this is because of the effect of the superposition of weight matrices.

In summary, the results of our simulations of Memory Capacity, Noise Tolerance and Processing Time show that QMAM has outstanding abilities compared to conventional methods.

## IV. System Architecture and Computational Intelligence for Robot Partner

### A. Communication System for Assocaitive Memory

We developed the interactive communication system with associative memory. Fig. 5(a) shows structure of the system. The system is composed of Robot Partner, Microsoft Kinect, Leap Motion [14], microphone and server PC. Kinect can get the RGB data and the distance data. Using inputs data that are received from Kinect, server PC detects the object color and shape by Steady-State Genetic Algorithm (SSGA), or

TABLE III: Processing Time Experimental Conditions

| | | | | | | | |
|---|---|---|---|---|---|---|---|
| Number of Pairs $k$ | | : | 1 to 300 Pairs (Non Duplicates) | | | | |
| Neuron Representation | | : | Bipolar | | | | |
| Data Set Configuration | | : | Random Pattern | | | | |
| Variation Amount $F$ | | : | 0.005 | | | | |
| | Layer No. | : | [1] | [2] | [3] | [4] | [5] |
| Number of Neurons | 5-Layers | condition (VI) | 15 | 14 | 13 | 12 | 11 |

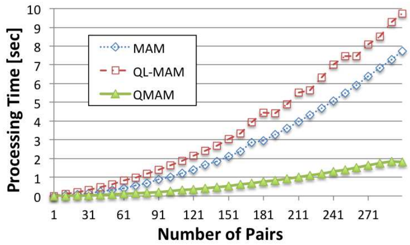


Fig. 4: Results of Processing Time with condition (VI).

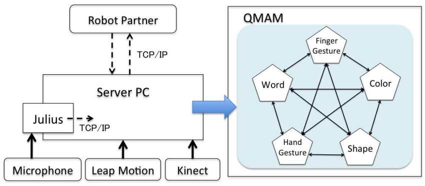


(a) The structure of robot system

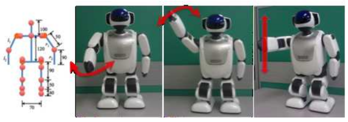

(b) Robot Partner behaviors (Lower Bye-Bye, Upper Bye-Bye and Up & Down).

Fig. 5: System Configuration and Robot Partenr.

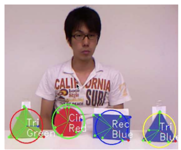

(a) Object Recognition

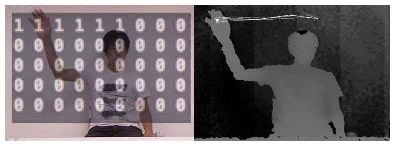

(b) Gesture Recognition

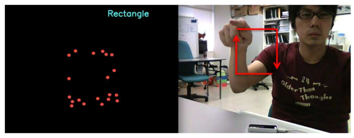


(c) Finger Gesture Recognition

Fig. 6: Example of Computational Intelligence for Recognition.

recognizes the hand gestures by Spiking Neural Networks (SNNs) [3]. Moreover, finger gestures are calculated by 3D finger position data from Leap Motion (Fig. 6). For voice recognition, we apply Julius that is open source large vocabulary continuous speech recognition engine [15]. It works in real time, and recognition accuracy shows over 90% in 20,000 words reading test. Microphone collects human voice for Julius. Server PC also calculates relationship between color, shape, hand gesture, word and finger gesture by QMAM. Then, based on the relationship, server PC sends the utterance or behavior order to Robot Partner by TCP/IP. Fig. 5(b) shows example of Robot behaviors.

### B. Multi-modal Communication with Robot Partner

Robot Partner with a human-like body and human-like abilities could in principle be capable of intuitive multimodal communication with human [3]. Moreover, it would be possible to transfer information while having effectiveness and robustness. Multiple modalities can be represented several information. Simultaneously, it can be supplemented such information with effective.

## V. Experimental Results

For this experiment, we defined 6 relationships with Color, Shape, Hand Gesture, Word and Finger Gesture as Table IV. Fig. 7(a) shows the sequentially input. Figs. 7(b), 7(c) and 7(d) show sequentially output of MAM, QL-MAM and QMAM, respectively. In Figs. 7(b) and 7(c), due to the low memory capacity, these cannot be stored any pattern pairs. In contrast, in Fig. 7(d), thanks to the large Memory Capacity and high recall reliability, output of QMAM shows the same waveform with input one. It means QMAM performs association correctly.

Fig. 8 shows the result of recall rate in each layer of QL-MAM and QMAM. Here, experimental condition is following as Tables IV and V. These results come from the first input of Fig. 7(a) (Finger Gesture input as ID 2). In Fig. 8(a), due to the set number of neurons is too small to store pattern, QL-MAM is converged to local minima. On the other hand, QMAM (Fig. 8(b)) shows a superior recall reliability.

From the results of this section, we can regard that QMAM is utility and effective method for associative communication system.

TABLE IV: Relationships between Color, Shape, Hand Gesture, Word and Finger Gesture information.

| ID | Relationship | | | | |
|---|---|---|---|---|---|
| | Color | Shape | Hand Gesture | Word | Finger Gesture |
| 0 | No Coloer | No Shape | No Gesture | No Word | No Finger Gesture |
| 1 | Red | Circle | Upper Right Circle | RED CIRCLE | Small Circle |
| 2 | Green | Triangle | Lower Bye-Bye | GREEN TRAIANGLE | Triangle |
| 3 | Blue | Rectangle | Upper Bye-Bye | BLUE RECTANGLE | Rectangle |
| 4 | Yellow | Circle | Upper Right Circle | YELLOW CIRCLE | Large Circle |
| 5 | Orange | Triangle | Lower Bye-Bye | ORANGE TRIANGLE | Triangle |

TABLE V: The number of neurons for Color, Object, Hand Gesture, Word and Finger Gesture.

| | Color | Shape | Hand Gesture | Word | Finger Gesture |
|---|---|---|---|---|---|
| The Number of Neurons: | 6 | 11 | 45 | 10 | 8 |

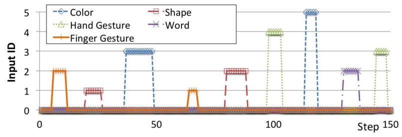


(a) Input ID

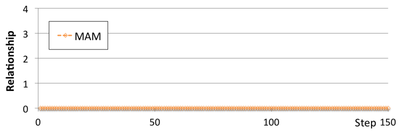


(b) MAM

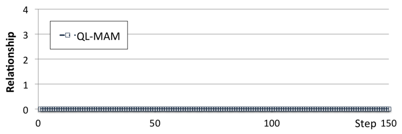


(c) QL-MAM

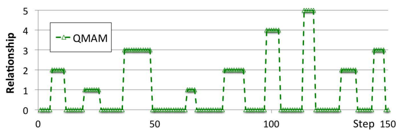


(d) QMAM

Fig. 7: The input ID and the result of output ID as Relationships.

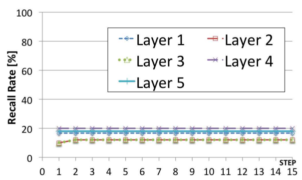


(a) QL-MAM

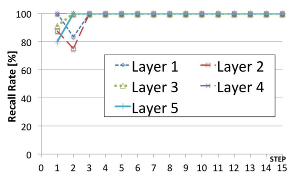


(b) QMAM

Fig. 8: The result of recall rate in each layer.

## VI. Conclusion

This paper has proposed a Quantum-Inspired Multidirectional Associative Memory, and discussed the capability of proposed model for human robot interaction. At first, We showed the structure of proposed model, and revealed similarity between Fuzzy inference and Quantum Mechanics, and proposed model satisfies two basic postulates of Quantum Mechanics. The results of simulation experiment show the proposed model has a superior ability. Moreover, the experimental results show proposed model can be applyed to interaction system with Robot Partner. In this paper, we defined relationships as arbitrarily.However, if we consider it with realistic, we regard that human can realize the mature communication with Robot Partner.

As future works, we will apply Complex-Valued Fuzzy logic to proposed model. It can be represented a oscillation, and this property is important factor of Quantum Mechanics. We expect that it can be extent a Memory Capacity and Noise Tolerance with Quantum Mechanics postulates.

## References


[1] D. Callahan, *Setting limits: medical goals in an aging society*. Georgetown University Press, 1995.

[2] E. Broadbent, R. Stafford, and B. MacDonald, "Acceptance of healthcare robots for the older population: review and future directions," *International Journal of Social Robotics*, vol. 1, no. 4, pp. 319–330, 2009.

[3] N. Kubota and Y. Toda, "Multimodal communication for human-friendly robot partners in informationally structured space," *Systems, Man, and Cybernetics, Part C: Applications and Reviews, IEEE Transactions on*, vol. 42, no. 6, pp. 1142–1151, 2012.

[4] M. Minsky, *The Society of Mind*. New York: Simon and Schuster, 1986.

[5] J. J. Hopfield, "Neural networks and physical systems with emergent collective computational abilities," *Proceedings of the National Academy of Sciences*, vol. 79, no. 8, pp. 2554–2558, 1982.

[6] B. Kosko, "Adaptive bidirectional associative memories," *Applied optics*, vol. 26, no. 23, pp. 4947–4960, 1987.

[7] M. Hagiwara, "Multidirectional associative memory," in *International Joint Conference on Neural Networks*, vol. 1, 1990, pp. 3–6.

[8] Y.-F. Wang, J. B. Cruz Jr, and J. H. Mulligan Jr, "Two coding strategies for bidirectional associative memory," *Neural Networks, IEEE Transactions on*, vol. 1, no. 1, pp. 81–92, 1990.

[9] H. Kang, "Multilayer associative neural networks (mann's): storage capacity versus perfect recall," *Neural Networks, IEEE Transactions on*, vol. 5, no. 5, pp. 812–822, 1994.

[10] H. Shi, Y. Zhao, and X. Zhuang, "A general model for bidirectional associative memories," *Systems, Man, and Cybernetics, Part B: Cybernetics, IEEE Transactions on*, vol. 28, no. 4, pp. 511–519, 1998.

[11] M. Hattori and M. Hagiwara, "Quick learning for multidirectional associative memories," in *Neural Networks, 1995. Proceedings., IEEE International Conference on*, vol. 4. IEEE, 1995, pp. 1949–1954.

[12] G. G. Rigatos and S. G. Tzafestas, "Quantum learning for neural associative memories," *Fuzzy Sets and Systems*, vol. 157, no. 13, pp. 1797–1813, 2006.

[13] D. J. Griffiths, *Introduction to quantum mechanics*. University Science Books, 1995.

[14] "Leap motion (https://www.leapmotion.com/)."

[15] A. Lee and T. Kawahara, "Recent development of open-source speech recognition engine julius," in *Proceedings: APSIPA ASC 2009*, 2009, pp. 131–137.